A NUMERICAL FRAMEWORK TO ANALYZE FRACTURE IN COMPOSITE MATERIALS: FROM SIMULATED CRACK RESISTANCE CURVES TO HOMOGENIZED SOFTENING LAWS

M. Herráez[1,2], C. González[1,2], C. S. Lopes[2]

[1]Departmento de Ciencia de Materiales, Universidad Politécnica de Madrid, 28040 Madrid, Spain
[2]IMDEA Materials, C/Eric Kandel 2, 28906 - Getafe, Madrid, Spain
Email: carlosdaniel.gonzalez@imdea.org, Web Page: http:// https://materiales.imdea.org

Keywords: Micro-mechanics, Fibre reinforced, Fracture, Finite element, Homogenization

Abstract
A numerical framework to obtain the crack resistance curve (R-curve) and its corresponding softening law for fracture analysis in composite materials under small scale bridging has been developed. The R-curve is computed for this material using a micromechanical embedded model corresponding to the intralaminar transverse tensile fracture toughness characteristic. The model combines an embedded cell approach with the Linear Elastic Fracture Mechanics (LEFM) displacement field to analyze the local crack growth problem including fiber/matrix interface debonding and matrix ligaments bridging as the main energy dissipation mechanisms. Parametric analysis were carried out to assess the influence of the properties of the material constituents on the R-curve behaviour and homogenized cohesive laws.

1. Micromechanical model

A simulation methodology was developed to infer the R-curve behaviour and investigate softening laws based on computational micromechanics to address crack propagation problems in unidirectional fiber reinforced composites [1]. The modeling strategy was applied to study the intralaminar transverse fracture toughness of a unidirectional UD carbon/epoxy system AS4/8552 using as inputs the micromechanical parameters and the reinforcement distribution. The model was only applied to study the bidimensional crack propagation assuming the matrix tearing and fiber/matrix interface debonding as the dominant energy dissipation mechanisms. Thus, other large scale effects due to fiber bridging were not taken into account in the model. The crack front is assumed to be parallel to the fiber direction, namely x and running in the plane y-z as shown in Figure 1. This propagation mode is also known as intralaminar propagation under transverse tension G_{2+}. The model includes the microstructure of the material, but, only in a small region close to the crack tip known as fracture process zone (FPZ). This methodology allows the isolation of the crack propagation problem from any global specimen geometry effect.

The microstructure used for the embedded region corresponds to a homogeneous dispersion of parallel fibers aligned in the x_1 direction, being the fiber volume fraction V_f=65%. The rest of the model, out of the embedded region, was treated as a homogeneous transversely isotropic elastic solid whose behaviour is given by any suitable homogenization scheme from the elastic constants of the constituents, fibers and matrix, and the volume fraction of reinforcement. The two regions of the model share the bounding nodes, so the displacement continuity is guaranteed. The width of the embedded model, h=100μm, was large enough to ensure the effect of the transition from heterogeneous to homogeneous solids induced negligible effects in the crack propagation process. The mesh size was set to 1μm in the embedded region and it progressively grows along the homogeneous region up to 480 μm at the outer edges. This discretization level ensures good representation of stress fields at the microlevel while maintaining acceptable computation times. A typical baseline model is formed by 385.000 elements. Simulations

were carried out using the implicit dynamic solver in Abaqus/Standard, the quasi-static solution settings and within the framework of the finite deformations theory with the initial unstressed state as the reference one.
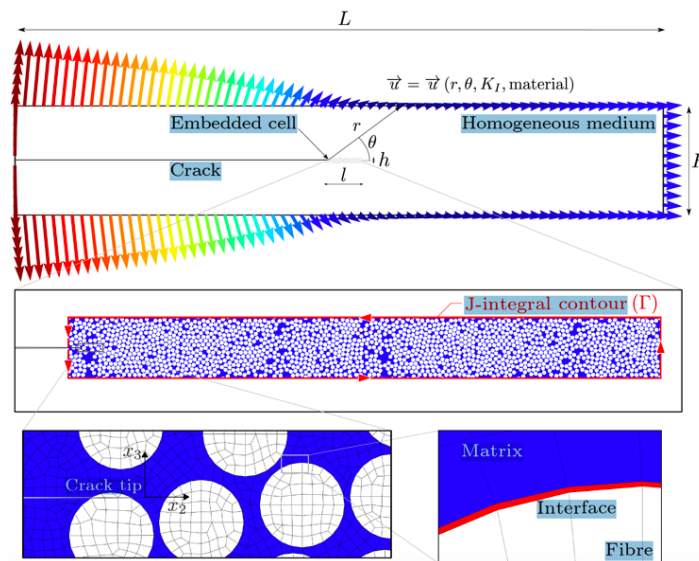
Figure 1. Schematic view of the model showing the detail of the fibres distribution, J-integral contour, FEM mesh, cohesive interface and displacement field (LEFM).

The model assumes that small scale bridging (SSB) conditions prevail, therefore, even if the stress field in the fracture process zone is affected by plasticity and/or damage, the overall stress in that area is dominated by the singular term $r^{-1/2}$ of the linear elastic fracture mechanics (LEFM). This condition is fulfilled if the characteristic length of the process zone is small as compared with the overall dimensions of the model and the crack tip is far from the model edges. Under such conditions, the K_I displacement field can be imposed in the outer region of the model to simulate a crack loaded in mode I conditions. This methodology is also known as boundary layer approach and is found in the literature for the analysis of the initiation and propagation of ductile cracks.

The model is loaded by increasing the stress intensity factor, K_I, until crack propagation Δa is observed. In most of the boundary layer models, the outer region where the displacement field is applied is significantly larger than the length of the propagated crack (L>> Δa), and thus, updating the displacement field due to crack tip propagation is not required. However, if the outer region is not large enough, a mismatch between the stress intensity factor imposed through the boundary conditions and the stress intensity factor measured in the vicinity of the crack tip is observed. The whole model was discretized using a lagrangian mesh with finite elements. The matrix, fibers and the homogenized region were modeled with 4-node fully integrated quadrilateral isoparametric plane strain elements (CPE4) in Abaqus/Standard. The fiber-matrix interface debonding was simulated with 4-node cohesive isoparametric elements (COH2D4) inserted at each of the individual fiber/matrix interfaces. The J integral along the Γ contour in Figure 1 was computed numerically from the results of the simulation in order to chech the consistency with the results obtained by imposing K_I on the boundaries.

Fibers were modeled as linear elastic transversely isotropic solids representative of a typical carbon fiber used in unidirectional reinforcements. The elastic properties corresponding to the homogenized medium out of the embedded region for V_f=65% volume fraction were determined by computational homogenization using FEM analysis of periodic representative volume element models in the elastic regime.

2. Homogenized cohesive laws

A homogeneous finite element model in which the fracture process zone is lumped into a single cohesive crack in the z plane was generated in order to evaluate the response of physically sound softening laws mimicking the response of the micromechanical model, Figure 3. In this case, the model is constructed with two homogeneous transversely isotropic elastic solids under plain strain conditions with same elastic constants and tied to a zero-thickness layer of cohesive elements. the total dimensions are the same than those of the embedded micromechanical model, lxh, using the same boundary conditions representing the displacement field of linear elastic fracture mechanics. The softening law $\sigma(w)$ used in the cohesive elements is defined with the strength, Y_t, toughness, G_f, and its shape (bilinear, exponential, etc.). As in the case of the elastic constants, the strength of the material, Y_t, was inferred using periodic representative volume elements. the remaining mechanical parameters are selected to reproduce the same $\Delta(a)$ response, in an energy release equivalence, as the embedded model containing the real material microstructure.
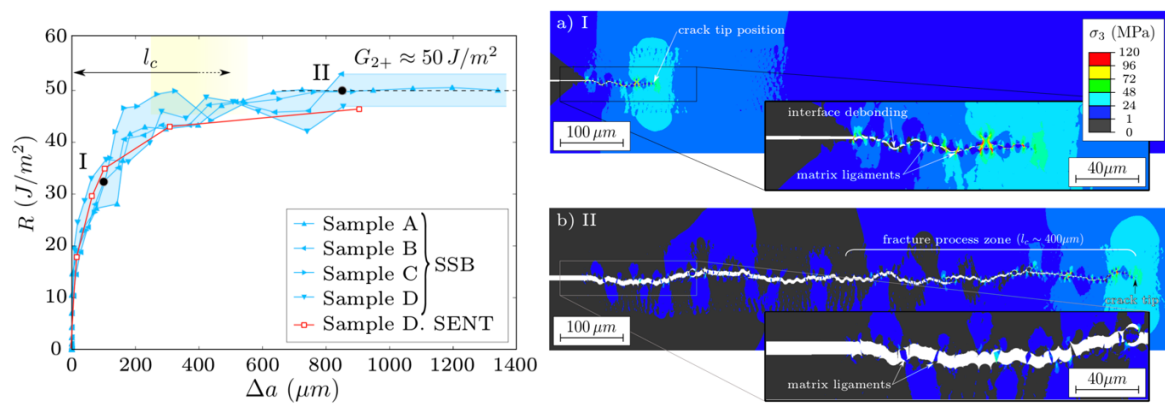

Figure 2. R-curve envelope obtained from four different equivalent realizations using the embedded boundary layer approach. Snap-shots of the fracture mechanisms obtained with the embedded microme- chanical model for the loading points I and II shown in the R(Δa).
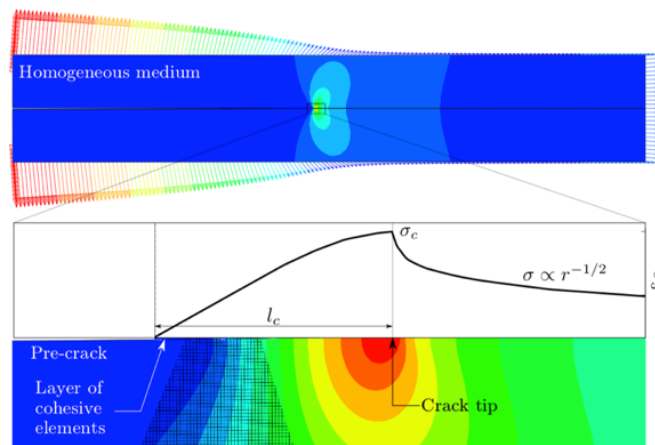
Figure 3. Sketch of the equivalent cohesive model for crack propagation, mode I displacement field is imposed in the boundaries of the model, and detail of the vertical stress contour field σ_3 of the homogeneous cohesive crack model along the fracture process zone with a linear-softening traction-separation law.

The homogenized model lumping the fracture process zone in a single layer of cohesive elements presented in Figure 3 is now applied to simulate the crack propagation problem. The maximum stress Y_t=50MPa was determined from the numerical simulation of a standard model based on the periodic representative volume element RVE of the microstructure subjected to uniaxial transverse tension loads for the same micromechanical properties of the constituents presented previously [2,3].

The fracture toughness G_{2+}=50J/m^2 was obtained from the embedded model Δa curve when steady-state conditions are achieved. Even if the two previously conditions are fulfilled, the shape of the σ(w) field presents an additional degree of freedom related with the shape of the R-curve.
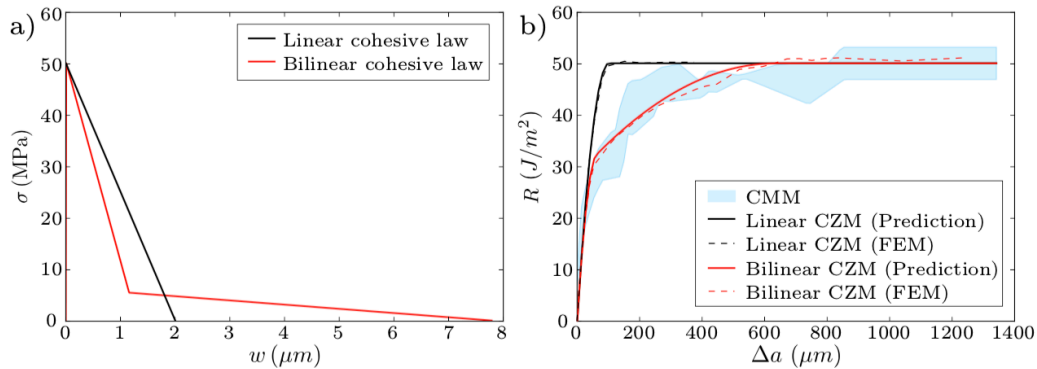

Figure 4. Linear and bilinear cohesive laws for homogenized models, b) Comparison of the R(Δa) curves obtained with the homogenized cohesive model using linear and bilinear laws with the micromechanics embedded cell approach.

To illustrate such effect, a standard linear-softening traction-separation law defined as $\sigma(w)=Y_t(1-w/w_c)$ with $w_c =2G_{2+}/Y_t$ is used (see figure 4a). The results of the homogenized cohesive model are presented in figure 4b). Naturally, the results match perfectly the steady-state toughness of the embedded model but the homogenized crack resistance curve does not fit the embedded cell model fracture response in the whole Δa range.

A non-conventional cohesive law is required to improve the fitting of the embedded model R-curve. Two well differentiated cohesive zones and fracture energies are observed in the R-curves (see figure 4). Hence, a bilinear softening law based on the work Davila [4], is proposed in order to capture the fracture process more accurately than the simple linear softening law previously shown. The bilinear softening law is described through the superposition of two linear cohesive laws, namely c1 and c2 with complimentary strength and fracture toughness values. The strength and toughness of the two superimposed cohesive laws are defined as fractions of Y_t and G_{2+}, respectively, as $\sigma_{c1}=nY_t$, $\sigma_{c2}=(1-n)Y_t$ and $G_1=mG_{2+}$ and $G_2=(1-m)G_{2+}$. Following this approach, the strength and toughness are directly obtained by the summation of the individual contributions of the linear cohesive laws as $Y_t= \sigma_{c1} +\sigma_{c2}$ and $G_{2+}=G_1+G_2$. The factors n and m range in the interval (0,1) and are used to control the shape of the bilinear cohesive law. They can be derived by least square minimization using the R(Δa) curves obtained with the micromechanical model. Not surprisingly, the results obtained with the bilinear cohesive law clearly fit the predicted R(Δa) curves in figure 4b) indicating the good representativeness of the fracture process zone by means of the bilinear softening law.

One of the main benefits of computational micromechanics is the ability to predict the mechanical behaviour of the composite material when the properties of the constituents are changed, and, thus, enabling the virtual optimization of the material prior to its manufacturing. The approach described previously is applied to determine the effect of the constituents, mainly the toughness of the fiber/matrix interface G_{int}, and the toughness of the matrix G_m, on the final homogenized behaviour of the UD composite material. Three different realizations with the same volume fraction V_f=65% were computed

using a set of values for G_{int}=2, 4, 6, 8, 10, 12, 15, 20J/m^2, and matrix, G_m=40, 80, 120, 200, 300J/m^2. The corresponding results of the R(Δa) curves are plotted in Figure 5b) and d), respectively, being the baseline values those obtained with G_{int}=2J/m^2 and G_m =90J/m^2 (plotted in light blue in the graph). The results indicate that a tough interface is critical to enhance energy dissipation, specially in the first stages of the process for small crack increments, as observed in Figure 5b). This effect can be attributed to the onset of damage that is triggered by fiber/matrix decohesion ahead of the notch tip. If fiber/matrix interface debonding is delayed, because of the higher G_{int}, then, more volume of material is able to contribute to dissipate energy in the neighborhood of the crack tip enhancing the fracture energy, and not only fibers close to the crack plane. Improving the interface toughness G_{int} from 2 to 20 J/m^2 produced an increase of the steady-state fracture energy from 50 to 175 J/m^2, Figure 5a). The simulations also point out that the influence of the matrix toughness on the steady-state fracture energy, G_{2+}, is not as effective as in the case of the fiber/matrix interface debonding, Figure 5b). For instance, changing the matrix toughness G_m from 40 to 300 J/m^{2}produces an improvement from 50 to 110 J/m^2. This effect is due to the damaged matrix ligaments that are less effective to shield the crack tip, so the effectiveness of improving the matrix toughness is only observed for larger crack propagation as compared with the fiber/matrix interface.
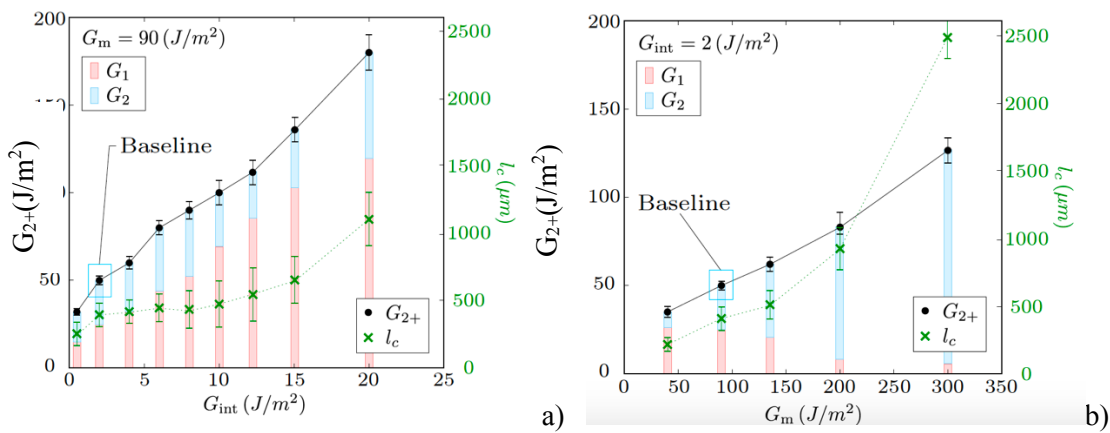
Figure 5. Steady-state toughness G_{2+}, G_1 and G_2 energy contributions, and fracture process length l_c for: a) interface toughness variations, c) matrix toughness variations. R(Δa) curves for: b) interface toughness variations, d) matrix toughness variations. The curves were obtained from fitting the numerical R(Δa) curves with the bilinear cohesive law.

3. Conclussions

The fracture behaviour of unidirectional fiber reinforced composite and the associated mechanisms were studied by means of computational simulation. A bidimensional modeling scheme was used to determine the interply fracture behaviour when a crack direction is perpendicular to the fiber direction and only accounts for fiber/matrix debonding and matrix plastic/damage mechanisms as the main contributions to the deformation and fracture mechanisms. Other important effects attributed to larger scale fiber bridging were not taken into account in the model as the characteristic length associated to them, of a few mm in length, is much larger than the close tip mechanisms studied in this work. Thus, the steady-state fracture toughness obtained following the methodology described in this paper should be understood as the crack tip toughness which is representative of effects operating at the micro scale.

The fracture behaviour was simulated by means of an embedded micromechanical model. Within this approach, the actual microstructure of the composite with the corresponding mechanisms was only included in the fracture process zone while the remaining model of size was assumed to be homogeneous with linear elastic behaviour. The mechanical properties associated to each of the constituents, fibers, matrix and interfaces, were reported in previous papers of the authors and were obtained from detailed

M. Herráez, C. González, C. S. Lopes

micromechanical experiments. Displacement fields associated with the K_I linear elastic fracture mechanics stress intensity factor were applied to external boundaries of the model and allowed to determine the R-curves under the small scale bridging conditions. In addition, a homogeneous model using cohesive elements introduced to track the crack propagation was developed in order to establish an energy equivalence with the micromechanical embedded approach. A bilinear homogenized cohesive law corresponding to fiber/matrix debonding and matrix damage/tearing was least-square fitted to the $R(\Delta a)$ results obtained with the embedded micromechanical model.

Acknowledgments

References

[1] M. Herráez, C. González, C.S. Lopes, A numerical framework to analyze fracture in composite materials: From R-curves to homogenized softening laws, International Journal of Solids and Structures, Volume 134, 2018, Pages 216-228, doi.org/10.1016/j.ijsolstr.2017.10.031.

[2] F. Naya, C. González, C.S. Lopes, S. Van der Veen, F. Pons, Computational micromechanics of the transverse and shear behavior of unidirectional fiber reinforced polymers including environmental effects, Composites Part A: Applied Science and Manufacturing, Volume 92, 2017, Pages 146-157, doi.org/10.1016/j.compositesa.2016.06.018.

[3] M. Herráez, C. González, C.S. Lopes, R. Guzmán de Villoria, J. LLorca, T. Varela, J. Sánchez, Computational micromechanics evaluation of the effect of fibre shape on the transverse strength of unidirectional composites: An approach to virtual materials design, Composites Part A: Applied Science and Manufacturing, Volume 91, Part 2, 2016, Pages 484-492, doi.org/10.1016/j.compositesa.2016.02.026.

[4] Dávila, C.G., Rose, C.A. & Camanho, P.P. A procedure for superposing linear cohesive laws to represent multiple damage mechanisms in the fracture of composites, Int J Fract (2009) 158: 211. https://doi.org/10.1007/s10704-009-9366-z